Desalination and Water Treatment
www.deswater.com
doi: 10.1080/19443994.2014.899521

54 (2015) 2314–2323
May

Taylor & Francis
Taylor & Francis Group

Flow-through experiments for bacteriophage MS2 removal by iron oxide-impregnated fiberglass

Jeong-Ann Park[a], Jae-Hyun Kim[a], Jin-Kyu Kang[a], Jeong-Woo Son[a], In-Geol Yi[a], Song-Bae Kim[a,b,*]

[a]*Environmental Functional Materials and Biocolloids Laboratory, Seoul National University, Seoul 151-921, Korea*
[b]*Department of Rural Systems Engineering and Research Institute for Agriculture and Life Sciences, Seoul National University, Seoul 151-921, Korea, Tel. +82 2 880 4587; Fax: +82 2 873 2087; email: songbkim@snu.ac.kr*

Received 5 September 2013; Accepted 18 February 2014

ABSTRACT

In this study, iron oxides were impregnated on the surface of fiberglass (Fe-fiberglass) to remove bacteriophage MS2 from water. The Fe-fiberglass was characterized using field emission scanning electron microscopy (FESEM), energy dispersive X-ray spectrometer (EDS), and X-ray diffractometry (XRD) analysis. The FESEM image showed that iron oxides covered the majority of the Fe-fiberglass surface as a heterogeneous layer. The EDS analysis indicated that the major elements of the Fe-fiberglass were oxygen (30.85 wt.%), carbon (28.61 wt.%), and iron (12.58 wt.%). The XRD pattern demonstrated that the iron oxides impregnated on the Fe-fiberglass were maghemite (γ-Fe_2O_3) and goethite (α-FeO(OH)). Flow-through column experiments were performed for chloride (Cl), a conservative tracer, and bacteriophage MS2 to quantify the bacteriophage removal by the Fe-fiberglass. The mass recoveries of Cl and MS2 in the raw fiberglass were 96.7 and 93.4%, respectively, indicating that the bacteriophage removal by the raw fiberglass was almost negligible. The mass recoveries of MS2 were 41.6–47.4% in the Fe-fiberglass, showing that the Fe-fiberglass was efficient in the removal of bacteriophage. In the presence of (bi)carbonate ions, the mass recovery of MS2 in the Fe-fiberglass was 63.1%, indicating that the bacteriophage removal could be reduced due to the competition for sorption sites between (bi)carbonate and bacteriophage. This study demonstrated that bacteriophage removal by fiberglass could be improved via the impregnation of iron oxides.

Keywords: Bacteriophage MS2; Fiberglass; Flow-through experiment; Iron oxide impregnation; Virus removal

1. Introduction

Viral contamination of surface water and groundwater is an environmental problem around the world that poses a great threat to human health. Inadequate sanitation causes waterborne diseases, leading to a great number of deaths, especially in developing countries [1,2]. Point-of-use (POU) water treatment alternatives are of considerable interest as they provide safe drinking water and subsequently prevent water-related diseases. POU treatment is directly applied to treat the water used at a single tap within a

*Corresponding Author.

home [3–5]. Researchers have coated filters, granular media, and membranes with iron (hydr)oxides to enhance the removal of viruses from water [6,7]. Raciny et al. [8] used polysulfone membranes coated with magnetite to remove bacteriophage MS2. Brown and Sobsey [9] removed the bacteriophages MS2 and PhiX174 from drinking water using ceramic filter materials amended with iron oxides.

Fiberglass is a fibrous material made of a plastic matrix reinforced by fine fibers of glass. It is widely used as fiber-reinforced polymer composites in industry because of its low cost, excellent insulating characteristics, good thermal properties, and high tensile strength [10,11]. Recently, fiberglass has been used as a matrix for the immobilization of iron oxides because it has a higher specific surface area than typical granular media (e.g. sand) [12]. The surface modification of fiberglass by functional materials for the removal of contaminants such as nitrate, atrazine, and arsenic has been reported by several researchers [13–15]. Nangmenyi and his colleagues [16,17] synthesized silver nanoparticle-impregnated fiberglass for the disinfection of water. They also coated silver-modified iron oxide nanoparticles on fiberglass to disinfect bacteria and viruses in water [18]. Gutierrez et al. [19] investigated the adsorption of bacteriophage MS2 and rotavirus to hematite (α-Fe_2O_3) coated onto fiberglass. More research is still necessary on the impregnation of fiberglass with iron oxides and the application of the modified fiberglass for virus removal from water.

In this study, iron oxide-impregnated fiberglass was prepared and characterized using field emission scanning electron microscopy (FESEM), energy dispersive X-ray spectrometer (EDS), and X-ray diffractometry (XRD) analysis. Flow-through column experiments were performed for chloride, a conservative tracer, and bacteriophage MS2. The breakthrough curves (BTCs) were obtained by monitoring effluent, and then, mass recoveries were quantified from these curves to determine the removal of bacteriophage from water. In addition, the modified dose–response kinetic model and one-dimensional transport model were used to analyze the BTCs obtained from the experiments and quantify the related model parameters.

2. Materials and methods

2.1. Preparation and characterization of iron oxide-impregnated fiberglass

Fiberglass obtained from Hyundai fiber, Korea, was used in the experiments. Before immobilization of the iron oxides, the fiberglass was thermally treated in an electric furnace (C-FMA; Vision Lab, Seoul, Korea) at 200˚C for 4 h to decompose a polyvinyl alcohol binder on the surface of the fiberglass [16]. An iron oxide suspension was prepared by the co-precipitation method. An alkali solution of sodium hydroxide (NaOH, 6 M) was added drop-wise into a 500-mL solution of $FeSO_4{\cdot}7H_2O$ (0.25 M) and $FeCl_3{\cdot}6H_2O$ (0.5 M) until it reached pH 7.6 with intensive stirring at room temperature. The suspension was sprayed onto the fiberglass to immobilize the iron oxides on its surface, and the impregnated fiberglass (Fe-fiberglass) was aged at 65˚C for 18 h. The resulting Fe-fiberglass was rolled around a glass rod (length = 10 cm; diameter = 0.75 cm), thermally treated again in the electric furnace at 150˚C for 6 h, washed with deionized water, and then dried at 65˚C for 16 h to obtain the final cartridge filters.

The Fe-fiberglass was characterized using FESEM, EDS, and XRD analysis. The FESEM and EDS (Supra 55VP, Carl Zeiss, Germany) analyses were used to visualize the Fe-fiberglass and quantify the elements of the Fe-fiberglass. The mineralogical and crystalline structural properties of the iron oxides and the Fe-fiberglass were examined using the XRD analysis (D8 Discover, Bruker, Germany) with a CuKα radiation of 1.5406 Å at a scanning speed of 0.6˚/sec.

2.2. Virus and plaque assays

The bacteriophage MS2 (ATCC 15597-B1) obtained from the American Type Culture Collection was grown on *Escherichia coli* (ATCC 15597) by the double-agar overlay method [20]. MS2 is a male-specific, undeveloped, icosahedral single-stranded RNA phage with a diameter of 24–26 nm and an isoelectric point of 3.9 [21]. Bacteriophages were enumerated by the plaque assay method using the *E. coli* host. Host culture (0.2 mL) and 0.1 mL of the diluted virus sample with 5 mL of soft agar were added to tubes, and the mixture was poured onto trypticase soy agar (TSA) plates to solidify. After solidifying, plates were incubated at 37˚C for 18 h.

2.3. Bacteriophage removal experiments

Preliminary experiments were conducted under batch conditions to examine the removal of bacteriophage MS2 by iron oxide nanoparticles (Fig. 1). MS2 stock solutions were diluted from a concentrated titer with artificial groundwater (AG; 0.075 mM $CaCl_2$, 0.082 mM $MgCl_2$, 0.051 mM KCl, 1.5 mM $NaHCO_3$, pH 7.6) to the desired concentration. The batch

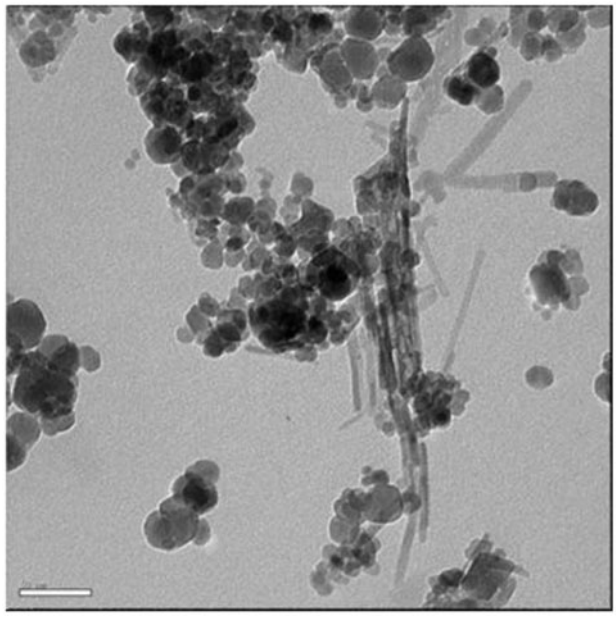

Fig. 1. Transmission electron microscopy image of iron oxide nanoparticles used in the batch experiments (bar = 50 nm).

experiments were performed with various doses of iron oxides (0.5, 1.0, 2.0, 3.0 g/L) with a reaction time of 4 h. The method consisted of adding virus stock solution (initial MS2 concentration = 6.01×10^5 pfu/mL) to centrifuge tubes containing iron oxides. After all of the tubes were properly prepared and sealed, they were shaken at 200 rpm for 4 h at 4℃ (IS-971R; Lab Company, Daejeon, Korea) to avoid thermal inactivation of the bacteriophage. The suspensions were then centrifuged at 9,000 × g and 4℃ for 15 min. (Combi-514R; Hanil Science Industrial, Incheon, Korea). The viable virus concentration was determined by the plaque assay method. Control tubes were filled with only virus solution and treated in the same manner as the experiment tubes. Virus removal was calculated with the following formula:

$$S = \left[\frac{C_i - C}{M}\right] \tag{1}$$

where S is the amount of virus removed per one gram of iron oxides (pfu/g), C_i and C are the initial and final virus concentrations, respectively, in the liquid phase (pfu/mL), and M is the total mass of iron oxides used in the experiment (g/mL).

Flow-through experiments were performed in a Plexiglas column (length = 10 cm; inner diameter = 2.5 cm) equipped with raw fiberglass and Fe-fiberglass cartridge filters (Fig. 2). The experimental conditions are summarized in Table 1. Prior to each experiment, the column was washed in 30% alcohol and thoroughly rinsed with deionized water. Then, the equipped column was flushed upward using an HPLC pump (Series II pump, Scientific Systems Inc., PA, USA) operating at a rate of 0.5 mL/min using 20 bed volumes of deionized water until steady-state flow conditions were established. Then, a solution of potassium chloride (KCl, 2 g/L) was continuously introduced downward into the column at the same flow rate. Portions of the effluent were collected using an auto collector (Retriever 500, Teledyne, City of Industry, CA, USA) at regular intervals. The effluent samples were analyzed for chloride concentration using a chloride probe (Orion 9617BNWP, Thermo Scientific Orion, NY, USA). Afterward, the column was flushed again with deionized water until no chloride was detected. Then, the bacteriophage MS2 (~10^5 pfu/mL) suspended in the artificial groundwater was continuously introduced into the column, and the effluent was collected in order to analyze the bacteriophage concentrations using the double-agar overlay method. All column experiments were conducted in a large refrigerator at approximately 4℃ to minimize the possible inactivation of the viruses due to high temperatures.

2.4. Data analysis

The total mass of bacteriophage injected into the column (M_{total}) during the experiment can be calculated as follows [22]:

$$M_{\text{total}} = C_0 Q t_{\text{total}} \tag{2}$$

where C_0 is the influent concentration of the bacteriophage, Q is the flow rate, and t_{total} is the total flow time. The column capacity for bacteriophage removal at a given flow rate and the influent concentration of bacteriophage (C_{cap}) can be quantified as follows:

$$C_{\text{cap}} = Q \int_{t=0}^{t=t_{\text{total}}} (C_0 - C_t)\mathrm{d}t \tag{3}$$

where C_t is the effluent concentration of the bacteriophage at time t. The mass recovery (M_r) of the bacteriophage during the experiment can be calculated as follows:

$$M_r = \left(1 - \frac{C_{\text{cap}}}{M_{\text{total}}}\right) \times 100 \tag{4}$$

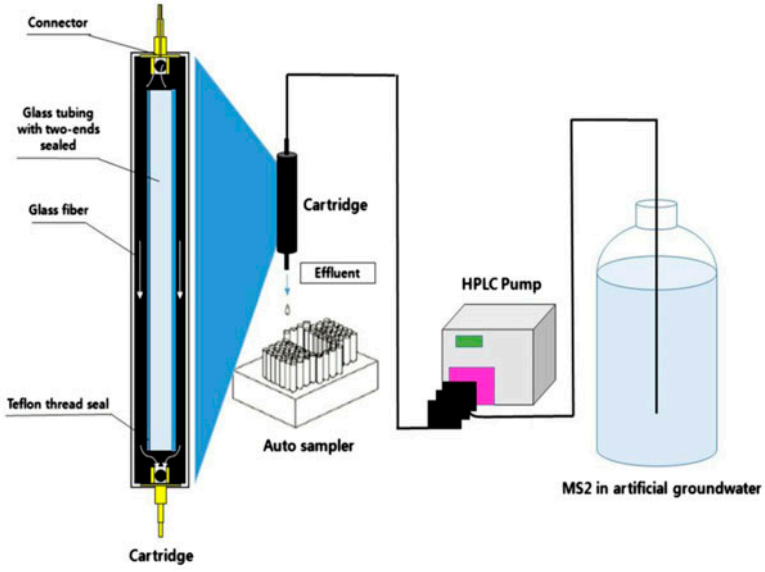

Fig. 2. Schematic diagram of the flow-through experiment (modified from Li et al. [30]).

Table 1
Flow-through column experimental conditions used in the study

Exp.	Filter materials	Solution	Solute	Solute concentration (g/L or PFU/mL)	Flow rate (mL/min)
1a	Raw fiberglass	DW	Chloride	2.0	0.5
1b	Raw fiberglass	AG	MS2	9.63×10^5	0.5
2a	Fe-fiberglass	DW	Chloride	2.0	0.5
2b	Fe-fiberglass	AG	MS2	4.25×10^5	0.5
3a	Fe-fiberglass	DW	Chloride	2.0	0.5
3b	Fe-fiberglass	AG	MS2	2.90×10^5	0.5
4a	Fe-fiberglass	DW	Chloride	2.0	0.5
4b	Fe-fiberglass	AG-10	MS2	7.43×10^5	0.5

Note: DW = deionized water; AG = artificial groundwater; AG-10 = AG with 10 mM $NaHCO_3$.

The mass of the bacteriophage removed per unit mass of adsorbent in the column (q_a), which is called the column capacity, can be determined as follows:

$$q_a = \frac{C_{cap}}{M_f} \tag{5}$$

where M_f is the mass of adsorbent in the column. The modified dose–response kinetic model can be presented as [23]:

$$\frac{C_t}{C_0} = 1 - \frac{1}{\left(\frac{C_0 Qt}{q_a M_f}\right)^A + 1} \tag{6}$$

where A is the modified dose–response model constant. The one-dimensional transport model for contaminants in the filter materials can be described as:

$$\frac{\partial C}{\partial t} = D\frac{\partial^2 C}{\partial x^2} - v\frac{\partial C}{\partial x} - \lambda C \tag{7}$$

where C is the concentration of the contaminants in the aqueous phase, D is the hydrodynamic dispersion coefficient, v is the velocity of the contaminants, and λ is the removal rate coefficient. The transport model parameters can be determined by fitting the CXTFIT code [24] to the BTCs of the contaminants.

3. Results and discussion

3.1. Characteristics of iron oxide-impregnated fiberglass

The FESEM images of the raw fiberglass and Fe-fiberglass are presented in Fig. 3. The raw fiberglass used in the experiments was balanced biaxial plain fabric (Fig. 3(a)). The individual fiber has a

diameter of 7.953 μm (Fig. 3(b)). In the Fe-fiberglass, iron oxides covered the majority of the fiberglass surfaces as a heterogeneous layer (Fig. 3(c)). Color mapping was performed to visualize the spatial distribution of iron (Fe) on the Fe-fiberglass as a red color (Fig. 3(d)).

The EDS analysis (Fig. 4(a)) indicated that the major elements of the Fe-fiberglass were oxygen (30.85 wt.%), carbon (28.61 wt.%), and iron (12.58 wt.%) along with other minor elements (silicon, calcium, etc.). Through the EDS analysis, iron (Fe) was found at the peak positions of 0.70, 6.40, and 7.06 keV as L-alpha, K-alpha, and K-beta X-ray signals, respectively. In addition, carbon (C) was evident at the peak position of 0.277 keV as the K-alpha X-ray signal.

The XRD pattern of the iron oxides (Fig. 4(b)) showed peaks corresponding to maghemite (γ-Fe_2O_3, JCPDS 89-5892, $2\theta = 30.266$, 35.651, 43.332, 53.766, 57.319, 62.949) and goethite (α-FeO[OH], JCPDS 81-0464, $2\theta = 21.240$, 33.243, 41.183, 58.998). The XRD pattern of the Fe-fiberglass also showed the major peaks found in iron oxides (Fig. 4(b)). Note that the goethite peaks were not noticeable on the Fe-fiberglass XRD pattern because the intensity of goethite peaks was far low relative to the peaks of others (halite, calcite, gypsum, etc.).

3.2. Bacteriophage MS2 sorption to iron oxide-impregnated fiberglass

The sorption of bacteriophage MS2 by iron oxides under batch experimental condition is presented in Table 2. The percent removal increased with an increasing dose of iron oxides from 0.5 to 3.0 g/L. At a dose of 0.5 g/L, the percent removal was 76.25 ± 0.62%. As the iron oxide dose increased to 1.0 g/L, the percent removal increased to 91.43 ± 1.07%. At 2.0 and 3.0 g/L, the percent removal further increased to 99.75 ± 2.60% and 99.90 ± 2.98%, respectively. Meanwhile, the removal capacity decreased with an increasing dose of iron oxides. At 0.5 g/L, the removal capacity was $(9.15 \pm 0.44) \times 10^8$ pfu/g. As the iron oxide dose increased to 1.0 g/L, the removal capacity decreased to $(5.49 \pm 0.03) \times 10^8$ pfu/g. At 2.0 and 3.0 g/L, the removal capacity further decreased to $(1.42 \pm 0.01) \times 10^8$ pfu/g and $(1.07 \pm 0.01) \times 10^8$ pfu/g, respectively. The batch tests demonstrated that iron oxides were effective in the removal of bacteriophage MS2.

The BTCs of chloride (Cl) and bacteriophage MS2 obtained from the flow-through column experiments are shown in Fig. 5. The experimental results of Cl and MS2 are presented in Tables 3 and 4, respectively. In the raw fiberglass column (Exp. 1), the effluent

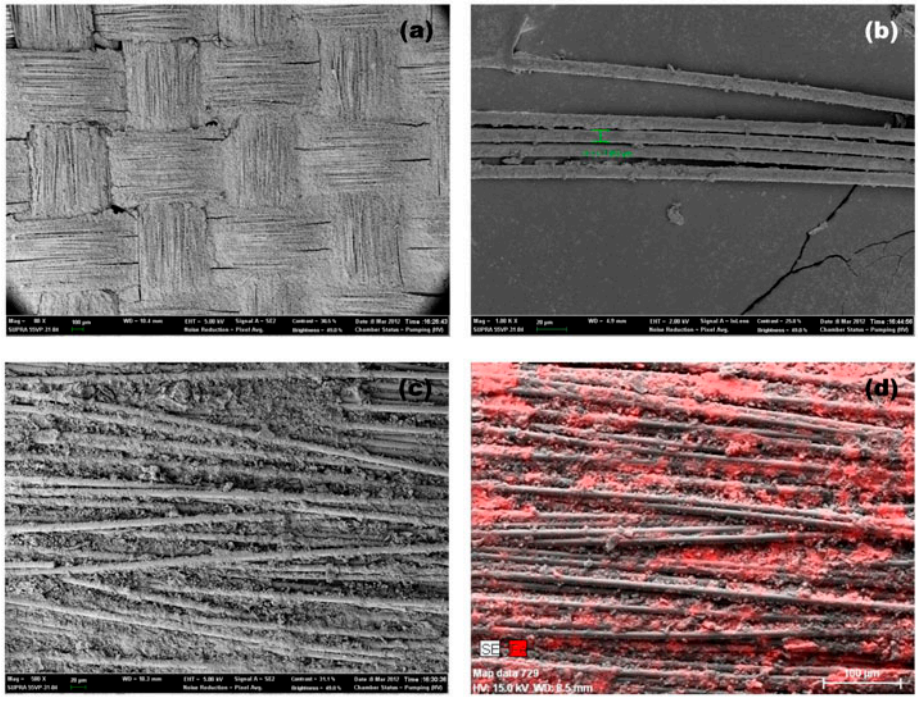

Fig. 3. FESEM images: (a) raw fiberglass (bar = 100 μm); (b) individual fiber (bar = 20 μm); (c) Fe-fiberglass (bar = 20 μm); (d) Fe color mapping of Fe-fiberglass (bar = 100 μm).

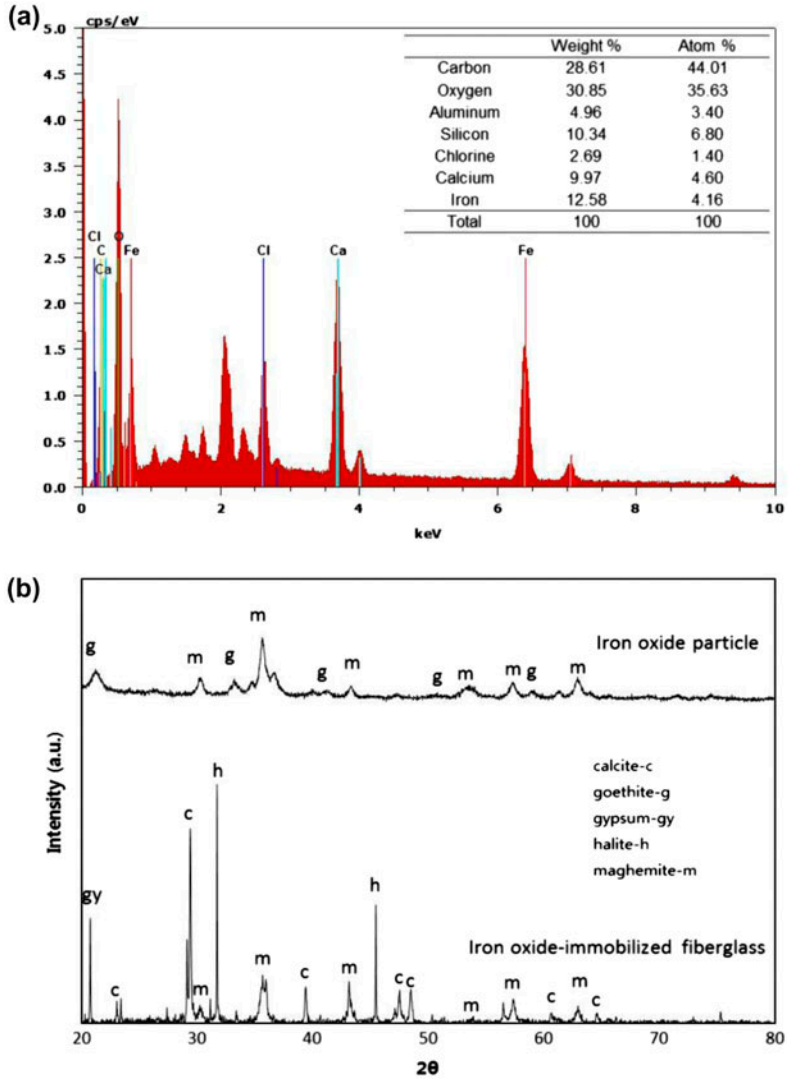

Fig. 4. EDS pattern of Fe-fiberglass (a) and XRD patterns of iron oxide particles and Fe-fiberglass (b).

Table 2
Removal of bacteriophage MS2 by iron oxide particles under batch experimental conditions (initial MS2 concentration = 6.01×10^5 pfu/mL; reaction time = 4 h)

Iron oxide dose (g/L)	0.5	1.0	2.0	3.0
Percent removal	76.25 ± 0.62	91.43 ± 1.07	99.75 ± 2.60	99.90 ± 2.98
Removal capacity ($\times 10^8$ pfu/g)	9.15 ± 0.44	5.49 ± 0.03	1.42 ± 0.01	1.07 ± 0.01

concentration of Cl, which is a conservative tracer, rose drastically with time and reached the influent concentration of Cl (relative concentration = 1.0) at 150 min. The effluent concentration of MS2 (Exp. 1) showed a similar trend with Cl, reaching the relative concentration of 1.0 at 150 min and then fluctuating between 0.75 and 1.09 (Fig. 5(a)). The mass recoveries of Cl and MS2 were 96.7 and 93.4%, respectively, indicating that the MS2 removal capacity of the raw fiberglass was very low.

Compared to the raw fiberglass, the Fe-fiberglass efficiently removed MS2 in the flow-through column

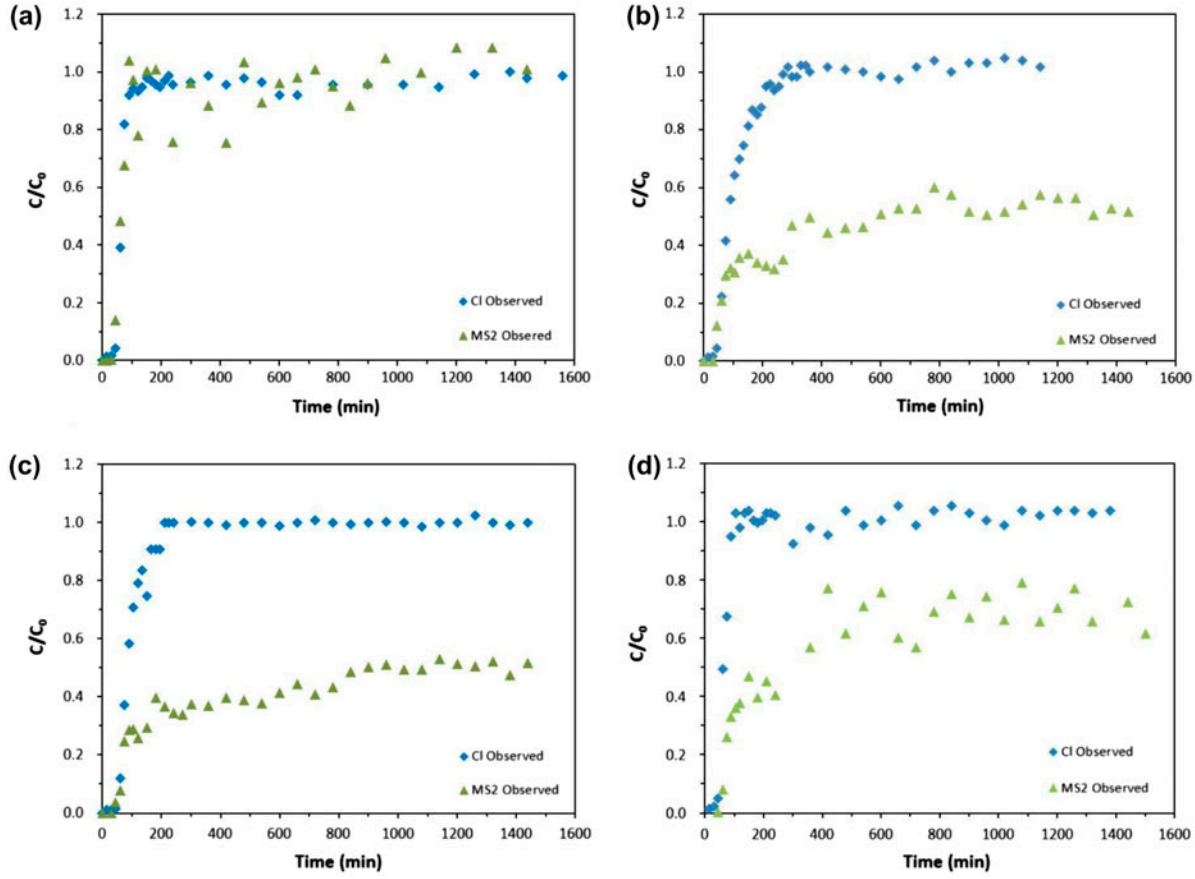

Fig. 5. Breakthrough curves of chloride (Cl) and bacteriophage MS2 obtained from flow-through column experiments: (a) Experiment 1 (raw fiberglass); (b) Experiment 2 (Fe-fiberglass); (c) Experiment 3 (Fe-fiberglass); (d) Experiment 4 (Fe-fiberglass). Experimental conditions are presented in Table 1.

Table 3
Column experimental results and model parameters obtained from chloride breakthrough curves

Exp.	M_r (%)	v (cm/min)	D (cm^2/min)	R^2
1a	96.7	0.158	0.036	0.981
2a	94.9	0.115	0.217	0.992
3a	97.2	0.114	0.127	0.988
4a	99.3	0.160	0.055	0.982

experiments. In the Fe-fiberglass columns (Exps. 2 and 3), the effluent concentration of Cl also rose drastically with time and reached the relative concentration of 1.0 at an early time. However, the effluent concentrations of MS2 (Exps. 2 and 3) showed different behaviors as compared to Cl, reaching a relative concentration of 0.4 around 200–300 min and then increasing slowly to 0.48–0.53 at 1,400 min (Fig. 5(b) and (c). The mass recoveries of Cl were 94.9 and 97.2% (Table 3), respectively, whereas the mass

Table 4
Column experimental results and model parameters obtained from bacteriophage MS2 breakthrough curves

Exp.	M_{total} (pfu)	C_{cap} (pfu)	M_r (%)	v (cm/min)	D (cm^2/min)	λ (1/min)	R^2
1b	6.93×10^8	4.54×10^7	93.4	0.163	0.071	3.0×10^{-4}	0.901
2b	3.06×10^8	1.61×10^8	47.4	0.092	4.319	1.9×10^{-3}	0.895
3b	2.09×10^8	1.22×10^8	41.6	0.066	2.621	2.0×10^{-3}	0.888
4b	6.91×10^8	2.55×10^8	63.1	0.073	0.735	1.5×10^{-3}	0.888

recoveries of MS2 were 47.4 and 41.6% (Table 4), respectively. These results indicated that the bacteriophage removal capacity of fiberglass could be enhanced through the impregnation of iron oxides on the surfaces of fiberglass.

In the case of Exp. 4, when 10 mM of $NaHCO_3$ was added to AGW, the bacteriophage removal capacity of the Fe-fiberglass was reduced. In the Fe-fiberglass columns (Exp. 4), the effluent concentration of Cl also showed the same trends as the cases of Exps. 1–3. The effluent concentration of MS2 also showed different behaviors as compared to Cl, reaching a relative concentration of 0.4 at 150 min and fluctuating between 0.41 and 0.79 thereafter (Fig. 5(d)). The mass recovery of Cl was 99.3% (Table 3), whereas the mass recovery of MS2 was 63.1% (Table 4). Compared to Exps. 2 and 3, the mass recovery of MS2 in Exp. 4 increased to 16–22%. This result could be attributed to the adsorption of (bi)carbonate ions to the surface of the iron oxides, resulting in a decrease of available sorption sites for MS2. (Bi)carbonate ions have great affinity for iron oxides and so disturb the adsorption of bacteriophage via the competition of sorption sites on the iron oxide surfaces. A similar finding was reported by Gutierrez et al. [19], who showed that no removal of MS2 and rotavirus by iron oxides (hematite) was observed in the presence of (bi)carbonate ions (0.1 and 1.0 mM). They reported that the virus removal was reduced because the sorption sites on the hematite surfaces were more preferentially occupied by (bi)carbonate than by viruses.

The modified dose–response model fits to the BTCs of MS2 are shown in Fig. 6. The observed BTCs were well described by the modified dose–response model. The model parameters for the modified dose–response model are summarized in Table 5. The modified dose–response model constants (A) in the Fe-fiberglass (Exps. 2b–4b) were in the range of 0.30–0.76, one order of magnitude larger than the value (= 6.58) in the raw fiberglass (Exp. 1b). The column capacity for MS2 removal determined from the model fitting ($q_{0,\mathrm{mod}}$) was similar to the value quantified from the experiments using Eq. (5) ($q_{0,\mathrm{exp}}$) (Table 5). The values of $q_{0,\mathrm{mod}}$ in the Fe-fiberglass (Exps. 2b–4b) were in the range of $(1.38–2.95)\times10^6$ pfu/g, one order of magnitude greater than the value ($=5.36\times10^5$ pfu/g) in the raw fiberglass (Exp. 1b).

The observed BTCs of Cl and MS2 are presented with the simulated BTCs from the transport model in Fig. 7. The observed BTCs of Cl indicated that the hydrodynamic conditions of the four column experiments were similar. For the BTCs of Cl (Fig. 7(a)), the transport characteristics v and D were determined to be 0.137 ± 0.026 cm/min and 0.109 ± 0.082 cm^2/min, respectively (Table 3). In addition, the values of v and D for the MS2 BTCs (Fig. 7(b)) were 0.099 ± 0.044 cm/min and 1.937 ± 1.921 cm^2/min, respectively (Table 4). The removal rate coefficients (λ) in the Fe-fiberglass (Exps. 2b–4b) were in the range of $(1.5–2.0)\times10^{-3}$ 1/min, which were one order of magnitude larger than the value in the raw fiberglass (3.0×10^{-4} 1/min; Exp. 1b).

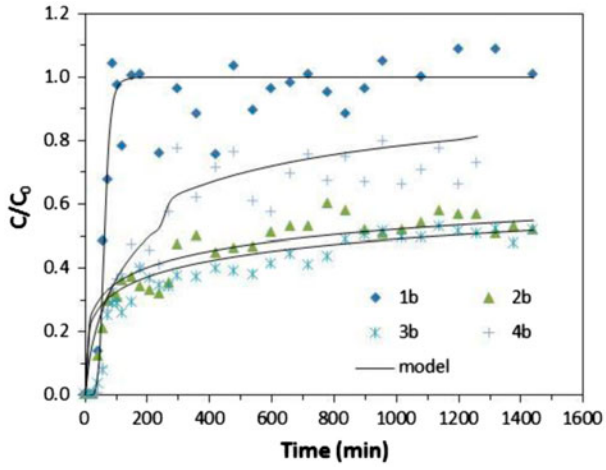

Fig. 6. Modified dose–response model fits to the breakthrough curves of bacteriophage MS2.

Table 5
Model parameters for modified dose–response model obtained from bacteriophage breakthrough curves

Exp.	A	$q_{a,\mathrm{mod}}$ (pfu/g)	$q_{a,\mathrm{exp}}$ (pfu/g)	R^2
1b	6.58	5.36×10^5	8.19×10^5	0.915
2b	0.30	2.86×10^6	2.91×10^6	0.887
3b	0.30	2.95×10^6	2.20×10^6	0.902
4b	0.76	1.38×10^6	1.60×10^6	0.901

3.3. Iron oxide-impregnated fiberglass and virus removal

In the literature, iron oxides have been impregnated on the surfaces of quartz sand to improve the virus removal capacity of the filter media [25,26]. Lukasik et al. [27] modified sand with iron oxides to remove poliovirus and bacteriophage MS2 from tap water. They reported from column experiments that modified sand efficiently removed viruses from water. Zhuang and Jin [28] examined the removal of two bacteriophages (PhiX174 and MS2) by goethite-coated sand using column experiments. They showed that solution chemistry (pH and anions) played a significant role in the removal of viruses by the coated sand.

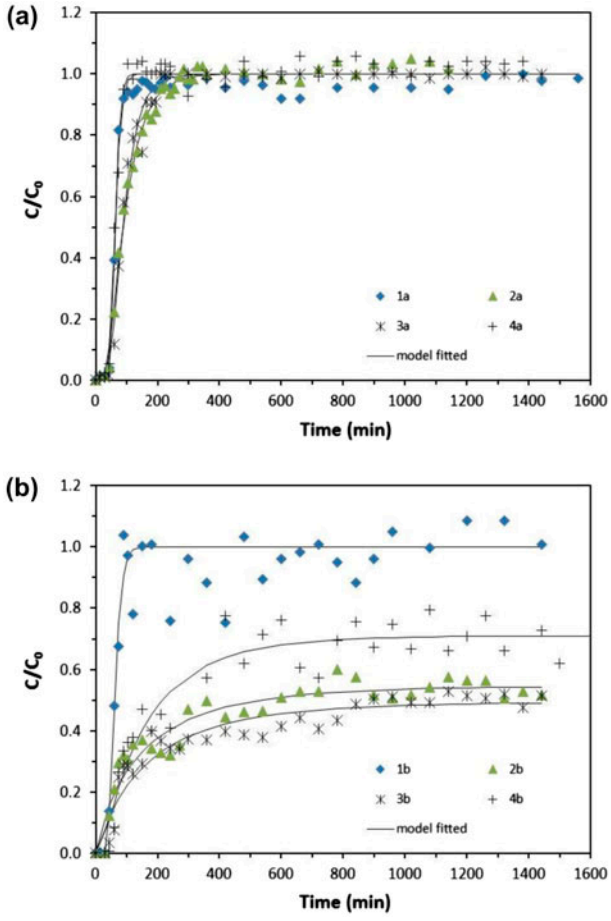

Fig. 7. Transport model fits to the breakthrough curves of (a) chloride (Cl); (b) bacteriophage MS2.

Bradley et al. [29] also performed column experiments using biosand filters amended with iron oxides to remove bacteriophage MS2. They reported that the iron-amended sand columns were far more effective in the removal of bacteriophage than the sand columns alone.

However, fiberglass has a higher specific surface area than sand due to its small diameter, so a higher loading of iron oxides on its surface can be achieved [12,15]. Recently, several studies have suggested that iron oxide-impregnated fiberglass may have advantages over iron oxide-impregnated sand in water treatments [15–17]. Kumar and colleagues [12,15] developed iron oxide-coated fibers and used them as adsorbents for arsenic removal in water. Li et al. [30] also developed an anionic exchange fiberglass with an iron oxide coating and used it as a POU device for arsenic removal in tap water. Nangmenyi et al. [16,17] observed the bactericidal activity of silver nanoparticle-impregnated fiberglass for water disinfection.

Furthermore, Nangmenyi et al. [18] modified iron oxide-impregnated fiberglass with silver nanoparticles to improve its antibacterial properties. They used the impregnated fiberglass for the removal of *E. coli* and bacteriophage MS2. Gutierrez et al. [19] examined the effective removal of rotavirus and bacteriophage MS2 by fiberglass impregnated with hematite nanoparticles through batch and flow-through experiments. They suggested that the iron oxide-impregnated fiberglass could be used as a POU device for virus removal. Our results also demonstrated the potential application of iron oxide-impregnated fiberglass for virus removal in water treatment.

4. Conclusions

Iron oxide-impregnated fiberglass was prepared and used for the removal of bacteriophage MS2 using flow-through experiments. In the raw fiberglass column, the BTC of MS2 showed a similar trend as the BTC of chloride. The mass recoveries of chloride and MS2 indicated that the bacteriophage removal capacity of the raw fiberglass was almost negligible. In the Fe-fiberglass columns, the BTCs of MS2 had a different behavior as compared to the BTCs of chloride. The mass recoveries indicated that the Fe-fiberglass was efficient in the removal of bacteriophage. In the presence of (bi)carbonate ions, the mass recovery of MS2 in the Fe-fiberglass increased, indicating that the bacteriophage removal was reduced due to the competition of sorption sites between (bi)carbonate and bacteriophage. This study demonstrated that the bacteriophage removal capacity of fiberglass could be improved via the impregnation of iron oxides. Further experiments are recommended to examine the simultaneous removal of viruses and other contaminants such as arsenic and fluoride from water using Fe-fiberglass as the filter materials.

Acknowledgments

This research was supported by the Korea Ministry of Environment as a GAIA project.

References

[1] B.A. Macler, J.C. Merkle, Current knowledge on groundwater microbial pathogens and their control, Hydrol. J. 8(1) (2000) 29–40.
[2] B.H. Keswick, C.P. Gerba, Viruses in groundwater, Environ. Sci. Technol. 14 (2000) 1290–1297.
[3] M.D. Sobsey, C.E. Stauber, L.M. Casanova, J.M. Brown, M.A. Elliott, Point of use household drinking water filtration: A practical, effective solution for pro-

viding sustained access to safe drinking water in the developing world, Environ. Sci. Technol. 42(12) (2008) 4261–4267.
[4] M.J. Slotnick, J.R. Meliker, J.O. Nriagu, Effects of time and point-of-use devices on arsenic levels in Southeastern Michigan drinking water, USA, Sci. Total Environ. 369(1–3) (2006) 42–50.
[5] S.A. Brownell, A.R. Chakrabarti, F.M. Kaser, L.G. Connelly, R.L. Peletz, F. Reygadas, M.J. Lang, D.M. Kammen, K.L. Nelson, Assessment of a low-cost, point-of-use, ultraviolet water disinfection technology, J. Water and Health 6(1) (2008) 53–65.
[6] I. Bradley, A. Straub, P. Maraccini, S. Markazi, T.H. Nguyen, Iron oxide amended biosand filters for virus removal, Water Res. 45(15) (2011) 4501–4510.
[7] J. Lukasik, Y.F. Cheng, F. Lu, M. Tamplin, S.R. Farrah, Removal of microorganisms from water by columns containing sand coated with ferric and aluminum hydroxides, Water Res. 33(3) (1999) 769–777.
[8] I. Raciny, K.R. Zodrow, D. Li, Q. Li, P.J.J. Alvarez, Addition of a magnetite layer onto a polysulfone water treatment membrane to enhance virus removal, Water Sci. Technol. 63 (2011) 2346–2352.
[9] J. Brown, M.D. Sobsey, Ceramic media amended with metal oxide for the capture of viruses in drinking water, Environ. Technol. 30(4) (2009) 379–391.
[10] S. Taj, M.A. Munawar, S. Khan, Natural-fiber-reinforced polymer composites, Proc. Pakistan Acad. Sci. 44(2) (2007) 129–144.
[11] P. Pozzi, R. Taurino, T. Zanasi, F. Andreola, L. Barbieri, I. Lancellotti, New polypropylene/glass composites: Effect of glass fibers from cathode ray tubes on thermal and mechanical properties, Composites Part A 41 (2010) 435–440.
[12] A. Kumar, P.L. Gurian, R.H. Bucciarelli-Tieger, C. Haas, G. Hsuan, Removal of Arsenic by Sorption to Iron-coated Fibers, Water Research Foundation and Arsenic Water Technology Partnership, Denver, CO, 2009.
[13] Y. Matatov-Meytal, V. Barelko, I. Yuranov, L. Kiwi-Minsker, A. Renken, M. Sheintuch, Cloth catalysts for water denitrification: II. Removal of nitrates using Pd–Cu supported on glass fibers, Appl. Catal. B 31(4) (2001) 233–240.
[14] Z. Yue, J. Economy, K. Rajagopalan, G. Bordson, M. Piwoni, L. Ding, V.L. Snoeyink, B.J. Mariñas, Chemically activated carbon on a fiberglass substrate for removal of trace atrazine from water, J. Mater. Chem. 16 (2006) 3375–3380.
[15] A. Kumar, P.L. Gurian, R.H. Bucciarelli-Tieger, J. Mitchell-Blackwood, Iron oxide-coated fibrous sorbents for arsenic removal, J. AWWA. 100 (2008) 151–164.
[16] G. Nangmenyi, Z. Yue, S. Mehrabi, E. Mintz, J. Economy, Synthesis and characterization of silver-nanoparticle-impregnated fiberglass and utility in water disinfection, Nanotechnology 20(49) (2009) 1–10.
[17] G. Nangmenyi, W. Xao, S. Mehrabi, E. Mintz, J. Economy, Bactericidal activity of Ag nanoparticle-impregnated fibreglass for water disinfection, J. Water Health 7(4) (2009) 657–663.
[18] G. Nangmenyi, X. Li, S. Mehrabi, E. Mintz, J. Economy, Silver-modified iron oxide nanoparticle impregnated fiberglass for disinfection of bacteria and viruses in water, Mater. Lett. 65(8) (2011) 1191–1193.
[19] L. Gutierrez, X. Li, J. Wang, G. Nangmenyi, J. Economy, T.B. Kuhlenschmidt, M.S. Kuhlenschmidt, T.H. Nguyen, Adsorption of rotavirus and bacteriophage MS2 using glass fiber coated with hematite nanoparticles, Water Res. 43(20) (2009) 5198–5208.
[20] M.H. Adams, Bacteriophages. Interscience Publishers, New York, NY, 1959.
[21] K.S. Zerda, Adsorption of viruses to charge-modified silica, PhD dissertation, Baylor College of Medicine, Houston, TX, 1982.
[22] H.C. Kim, S.J. Park, C.G. Lee, Y.U. Han, J.A. Park, S.B. Kim, Humic acid removal from water by iron-coated sand: A column experiment, Environ. Eng. Res. 14(1) (2009) 41–47.
[23] G. Yan, T. Viraraghavan, M. Chen, A new model for heavy metal removal in a biosorption column, Adsorpt. Sci. Technol. 19(1) (2001) 25–43.
[24] N. Toride, F.J. Leij, M.T. van Genuchten, The CXTFIT code for estimating transport parameters from laboratory or field tracer experiments, Research Report No. 137. US Salinity Laboratory, 1995.
[25] D. Schulze-Makuch, R.S. Bowman, S.D. Pillai, H. Guan, Field evaluation of the effectiveness of surfactant modified zeolite and iron-oxide-coated sand for removing viruses and bacteria from ground water, Ground Water Monit. Rem. 23(4) (2003) 68–74.
[26] B.M. Pecson, L. Decrey, T. Kohn, Photoinactivation of virus on iron-oxide coated sand: Enhancing inactivation in sunlit waters, Water Res. 46(6) (2012) 1763–1770.
[27] J. Lukasik, Y.F. Cheng, F. Lu, M. Tamplin, S.R. Farrah, Removal of microorganisms from water by columns containing sand coated with ferric and aluminum hydroxides, Water Res. 33(3) (1999) 769–777.
[28] J. Zhuang, Y. Jin, Interactions between viruses and goethite during saturated flow: Effects of solution pH, carbonate, and phosphate, J. Contam. Hydrol. 98(1–2) (2008) 15–21.
[29] I. Bradley, A. Straub, P. Maraccini, S. Markazi, T.H. Nguyen, Iron oxide amended biosand filters for virus removal, Water Res. 45(15) (2011) 4501–4510.
[30] X. Li, J. Wang, J. Economy, W.R. Kelly, Development of an anionic exchange glass fiber substrate POU device to remove arsenic, Final Report Midwest Technology Assistance Center, Illinois, USA, 2009.